

## Supplemental material on "Mechanical stress relaxation in molecular self-assembly"

Lucas Menou and Martin Castelnovo  
*Univ Lyon, Ens de Lyon, Univ Claude Bernard,  
 CNRS, Laboratoire de Physique, F-69342 Lyon, France*  
 (Dated: June 11, 2019)

In this supplemental material, we provide complementary informations to our main article. This covers three aspects: the comparison between stress relaxation pattern when defects are arranged along a single radial direction, or along multiple radial directions, the evolution of stress relaxation pattern for scars of different length, and finally self-assembly simulation results showing the appearance of dislocation instead of disclination by tuning the difference between heptagon and pentagon threshold  $\sigma_{7c} - \sigma_{5c}$ .

### I. DEFECTS ALONG ONE DIRECTION VERSUS MULTIPLE DIRECTIONS

In this section, we use the model described in the main text of this work in order to compute the hoop stress at the rim of the assembly for two scenarii: (i) all defects are present along a single radial direction (figure 1a), and (ii) all defects are present along multiple directions (figure 1b). The quantitative comparison between the two situations

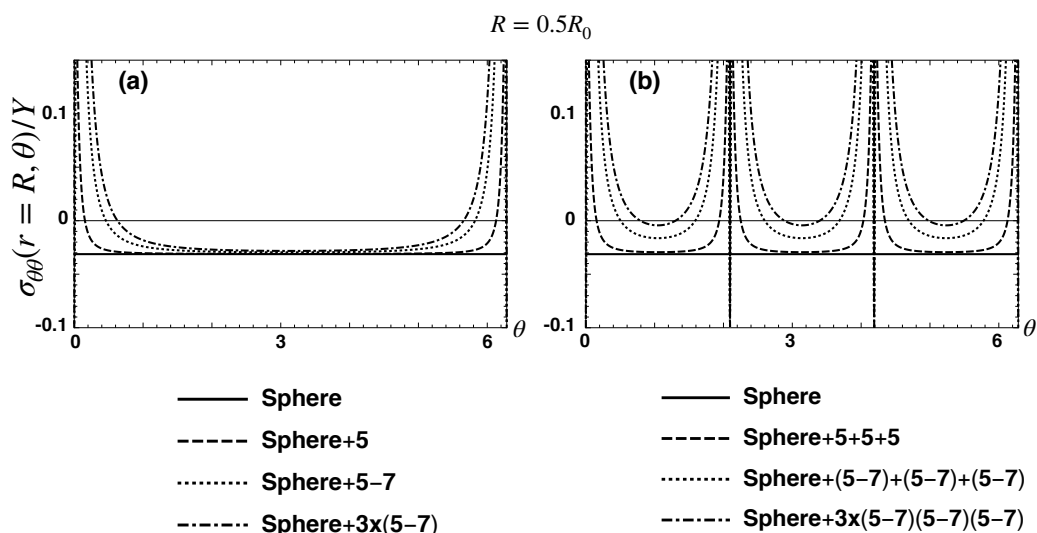


FIG. 1: Hoop stress at the rim of the assembly as function azimuthal angle  $\theta$ . (a) Defects are localized along a single direction. Various defect distribution are considered: single disclination ( $\rho_1 = 4.75R$ ), single dislocation ( $\rho_1 = 4.75R$ ), scar of three dislocations ( $\rho_1 = 0.95R, \rho_2 = 0.97R, \rho_3 = 0.99R$ ). (b) Defects are localized along three directions ( $\theta = 0, 2\pi/3$  and  $4\pi/3$ ). Radial positions are similar to (a). Other parameters:  $R/R_0 = 0.5$

with defects which are localized at same radial positions shows that the stress relaxation pattern is enhanced in the presence of multiple directions. This is easily understood by the fact that more defects are present in the latter case, suggesting an increased relaxation effect. Moreover, we observe that the order of the curves is conserved in single and multiple directions: the best relaxation configuration among the three tested is the scar, then the single dislocation, and finally the single disclination. These results justify our strategy of single direction comparisons in order to understand the features of stress relaxation pattern by defect nucleation.

## II. EFFECT OF SCAR LENGTH ON HOOP STRESS RELAXATION PATTERN

In this section, we used the elastic model in order to compare the hoop stress at the rim of the assembly, when radial scars of different length are used along a single direction. We used scars made of three, five, ten and fifteen dislocations (figure 2). This figure shows two results: first increasing the length of the scar leads to better stress relaxation, as it is observed from the vertical shift of the stress towards more tensile (positive) hoop stresses. Second, in order to achieve the best relaxation, the scar has to start in the bulk and to end at the boundary. In particular, if the scar ends before the boundary, the stress relaxation is not optimal within the configurations tested here.

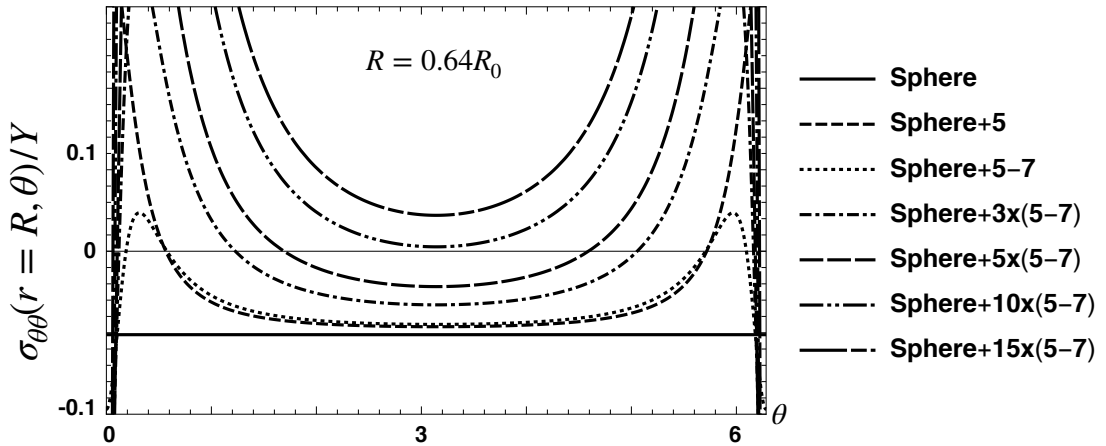


FIG. 2: Hoop stress at the rim of the assembly as function azimuthal angle  $\theta$ . Defects are localized along a single direction. Various defect distribution are considered: single disclination ( $\rho_1 = 0.758R$ ), single dislocation ( $\rho_1 = 0.758R$ ), scars of multiple dislocations (3, 5, 10, 15) with positions  $\rho_1 = 0.758R, \rho_2 = 0.766R, \rho_3 = 0.773R, \rho_4 = 0.781R, \rho_5 = 0.789R, \rho_6 = 0.797R, \rho_7 = 0.805R, \rho_8 = 0.813R, \rho_9 = 0.820R, \rho_{10} = 0.828R, \rho_{11} = 0.836R, \rho_{12} = 0.844R, \rho_{13} = 0.852R, \rho_{14} = 0.859R, \rho_{15} = 0.867R$ . Other parameters:  $R/R_0 = 0.64$

## III. SWITCHING FROM DISCLINATION TO DISLOCATIONS UPON ASSEMBLY

In this section, we present results of self-assembly simulation. The algorithm is very similar to the one used in the group of Roya Zandi [1–4]. We summarize here its main features, and the modifications we brought to the algorithm. The building blocks of the simulation are deformable triangles that self-assemble by sharing some edges. The elastic energy (Eq. 18 of the main text) of the growing surface contains an harmonic term associated to each triangle edge (therefore assimilated as regular springs), and a bending term associated with the angle between the normal vectors of neighboring triangle. At each growing step of the simulation, the energy is optimized using conjugate gradient method. In the original algorithm, each time five triangles meet at a common vertex, there is choice to be made: closing the pentagon or adding a new triangle and closing the hexagon. The choice can be made based on energetic

criterion for example, the configuration chosen being the one with lowest elastic energy. Equivalently, the choice can be made by comparing the length between free vertices of the configuration. If this length is smaller than a threshold value  $l_{5c}$ , the local structure is closed into a pentagon. If it is larger than this value, a triangle is added and the local structure is closed into an hexagon. In our algorithm, we modified this last step. Indeed, in the main text of the article, we suggested (Figure 1 of main text) that, depending on the value of hoop stress, the local structure is to be closed into a pentagon, hexagon or heptagon. Using the classical Hooke relation (Eq. 9 and 10 from main text), we can translate the stress thresholds  $\sigma_{5c}$  and  $\sigma_{7c}$  into strain thresholds  $u_{5c} = \sigma_{5c}/Y$  and  $u_{7c} = \sigma_{7c}/Y$  at the rim of the assembly. Now these critical strains can be translated into length thresholds simply by writing  $u_{5c} = (l_{5c} - l_0)/l_0$  for example. Therefore, in the simulation, we associate two length thresholds  $l_{5c}$  and  $l_{7c}$  with the mechanism of local structure closure.

As a consequence, the local closure rule goes as follows: when the length between free vertices is smaller than  $l_{5c}$ , the local structure is closed into a pentagon; when it is between  $l_{5c} < l < l_{7c}$ , the structure is closed into an hexagon (one triangle is added) ; when it is larger than  $l_{7c}$ , the structure is closed into an heptagon (two triangles are added). The results of the simulations are shown in figure 3 for different values of  $l_{7c}$ , but with the same value of  $l_{5c}$ . It is observed that reducing the length threshold  $l_{7c}$  promotes the transition from disclination-only mode of stress relaxation to dislocations and scars-only mode of relaxation. Therefore these data illustrate within a numerical

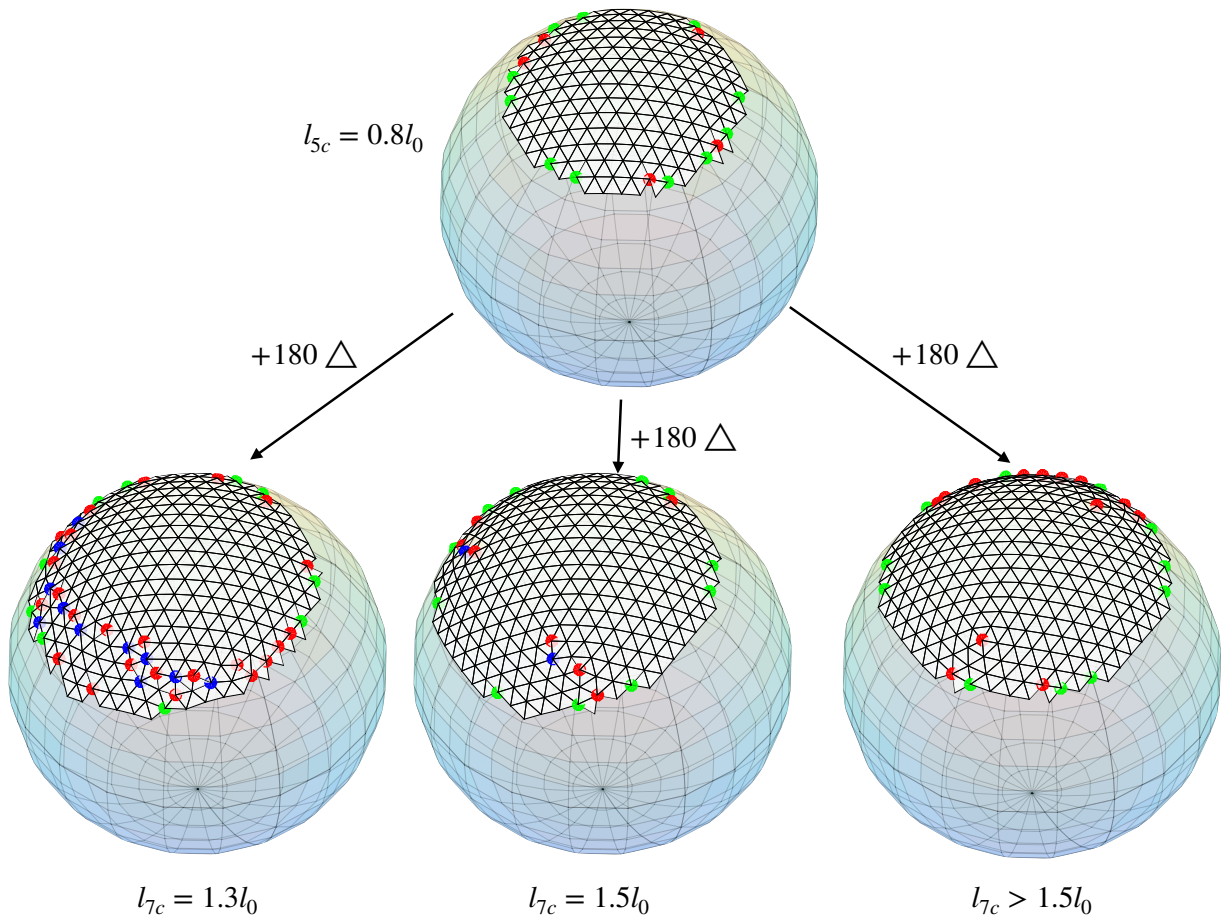


FIG. 3: Early steps of self-assembly showing the nucleation of the first defect depending on the value of hoop stress threshold. The first closing threshold is associated the length  $l_{5c} = 0.8l_0$ . (*Top*) The lowest configuration correspond to a defect-free surface. Adding 180 additional triangles leads to three types of configurations, depending on the value of the second threshold  $l_{7c}$ : (*right*) the first defect is a disclination for  $l_{7c} > 1.5l_0$ ; (*center*) the first defect is a dislocation (*i.e.* two disclinations 5 and 7) for  $l_{7c} = 1.5l_0$  for example; (*left*) the first defect are scars (multiple dislocations) for  $l_{7c} = 1.3l_0$  for example. Other parameters:  $k_e/k_b = 100$ ,  $R_0 = 10l_0$

experiment the mechanism of defect nucleation based on hoop stress threshold at the rim that is proposed within the main text. In addition to this last figure, we provide as a supplement three videos showing the self-assembly process for disclination, dislocation and scar dominated stress relaxation.

#### IV. LEGEND OF THREE VIDEO FILES

- File named *Construction-disclination.avi* This video file contains snapshots of assembly for parameters for which disclinations are the first isolated defect to appear. Green dots are localized at vertices with coordination four, red dots are localized at vertices with coordination five, blue dots are localized at vertices with coordination seven.
- File named *Construction-dislocation.avi* This video file contains snapshots of assembly for parameters for which dislocations are the first isolated defect to appear. Green dots are localized at vertices with coordination four, red dots are localized at vertices with coordination five, blue dots are localized at vertices with coordination seven.
- File named *Construction-scars.avi* This video file contains snapshots of assembly for parameters for which scars are the first combined defects to appear. Green dots are localized at vertices with coordination four, red dots are localized at vertices with coordination five, blue dots are localized at vertices with coordination seven.

- 
- [1] S. D. Hicks and C. L. Henley, Phys. Rev. E **74**, 031912 (2006).  
[2] A. Levandovsky and R. Zandi, Phys. Rev. Lett. **102**, 198102 (2009).  
[3] J. Wagner and R. Zandi, Biophys. J. **109**, 956 (2015).  
[4] S. Li, P. Roy, A. Travasset, and R. Zandi, Proc. Nat. Acad. Sci. **115**, 10971 (2018).